

FINAL REPORT

Magnetic Sensors with Picotesla Magnetic Field Sensitivity at Room Temperature

SERDP Project MM-1569

June 2008

Sy-Hwang Liou
University of Nebraska
Department of Physics and Astronomy and
Nebraska Center for Materials and Nanosciences

This document has been approved for public release.



Strategic Environmental Research and
Development Program

Report Documentation Page

Form Approved
OMB No. 0704-0188

Public reporting burden for the collection of information is estimated to average 1 hour per response, including the time for reviewing instructions, searching existing data sources, gathering and maintaining the data needed, and completing and reviewing the collection of information. Send comments regarding this burden estimate or any other aspect of this collection of information, including suggestions for reducing this burden, to Washington Headquarters Services, Directorate for Information Operations and Reports, 1215 Jefferson Davis Highway, Suite 1204, Arlington VA 22202-4302. Respondents should be aware that notwithstanding any other provision of law, no person shall be subject to a penalty for failing to comply with a collection of information if it does not display a currently valid OMB control number.

1. REPORT DATE 01 JUN 2008		2. REPORT TYPE N/A		3. DATES COVERED -	
4. TITLE AND SUBTITLE Magnetic Sensors with Picotesla Magnetic Field Sensitivity at Room Temperature				5a. CONTRACT NUMBER	
				5b. GRANT NUMBER	
				5c. PROGRAM ELEMENT NUMBER	
6. AUTHOR(S)				5d. PROJECT NUMBER	
				5e. TASK NUMBER	
				5f. WORK UNIT NUMBER	
7. PERFORMING ORGANIZATION NAME(S) AND ADDRESS(ES) University of Nebraska Department of Physics and Astronomy and Nebraska Center for Materials and Nanosciences				8. PERFORMING ORGANIZATION REPORT NUMBER	
9. SPONSORING/MONITORING AGENCY NAME(S) AND ADDRESS(ES)				10. SPONSOR/MONITOR'S ACRONYM(S)	
				11. SPONSOR/MONITOR'S REPORT NUMBER(S)	
12. DISTRIBUTION/AVAILABILITY STATEMENT Approved for public release, distribution unlimited					
13. SUPPLEMENTARY NOTES The original document contains color images.					
14. ABSTRACT					
15. SUBJECT TERMS					
16. SECURITY CLASSIFICATION OF:			17. LIMITATION OF ABSTRACT	18. NUMBER OF PAGES	19a. NAME OF RESPONSIBLE PERSON
a. REPORT unclassified	b. ABSTRACT unclassified	c. THIS PAGE unclassified			

This report was prepared under contract to the Department of Defense Strategic Environmental Research and Development Program (SERDP). The publication of this report does not indicate endorsement by the Department of Defense, nor should the contents be construed as reflecting the official policy or position of the Department of Defense. Reference herein to any specific commercial product, process, or service by trade name, trademark, manufacturer, or otherwise, does not necessarily constitute or imply its endorsement, recommendation, or favoring by the Department of Defense.

Table of Contents

Abstract	4
Tables	5
Figures	5
1. Introduction	6
2. Fabrication of magnetoresistive sensor	6
3. Magnetic sensor sensitivity	11
4. Summary	14
5. References	15
6. Appendices	16

Acronyms:

MEC- munitions and explosives of concern

MTJ - magnetic tunneling junction

pT - the picotesla (10^{-12} tesla)

SQUID - Superconducting quantum interference device

MFC - magnetic flux concentrators

RA - resistance time area

ΔR - the change in resistance

AFM – Antiferromagnetic

FM – ferromagnetic

MR – magnetoresistance

Magnetic Sensors with Picotesla Magnetic Field Sensitivity at Room Temperature SERDP SEED Project MM-1569, Principal Investigator: Sy-Hwang Liou

Abstract

High sensitivity magnetic sensors will have a significant impact on security, industry, and quality of life. Many of these applications require sensitivities better than $1 \text{ nT/Hz}^{1/2}$ as well as low cost, small size, low maintenance, and low power consumption. This project is to develop highly sensitive magnetic sensors that fit the goal of the MMSO-07-03 Statement of Need. This need is to develop novel sensors applicable to the diverse detection and discrimination problems of munitions and explosives of concern (MEC) contaminated sites.

We present a design of a low power, compact, magnetoresistive sensor. The key features of the design are (1) decreasing the noise by the use of a 64 element bridge, (2) reducing the magnetic noise by annealing of MTJ in high magnetic field and a hydrogen environment, and (3) increasing signal by the use of external low-noise magnetic flux concentrators. The field noise of our prototype magnetic sensor are approximately $1 \text{ pT/Hz}^{1/2}$ at 1 kHz, $5 \text{ pT/Hz}^{1/2}$ at 10 Hz, and $50 \text{ pT/Hz}^{1/2}$ at 1 Hz at room temperature. The magnetic sensor only dissipates 15 mW of power while operating.

Tables

Table 1 The estimated gains of various MFCs at gape of 1 mm

Figures

Fig. 1 (a) 64 element symmetric configuration (b) 64 element asymmetric configuration
Arrows in the graph indicate the reference layer pinning direction.

Fig. 2 The structure of the magnetic tunnel junctions (MTJs) is 5 nm Ta / 5 nm Cu / 10 nm Ir₂₀Mn₈₀ / 2 nm Co₉₀Fe₁₀ / 0.85 nm Ru / 3 nm Co₆₀Fe₂₀B₂₀ / 1.4 nm Al₂O₃ / 2 nm Co₉₀Fe₁₀ / 28 nm Ni₈₀Fe₂₀ / 5 nm Ta / 5 nm Ru. The junctions were patterned into ellipses with a size of 13.3 μm x 20 μm (area 209 μm², eccentricity 0.75). They were configured into a 64 element asymmetric configuration bridge. Solid arrows in the micrograph indicate the reference layer pinning direction for an asymmetric bridge and dotted arrows show the pinning direction for a symmetric bridge. The red arrow is the applied magnetic field direction

Fig. 3 (a) The R vs. H curve of the MTJ bridge with junction size 5 μm x 7.5 μm annealed at 265°C under fields of 7 T and 0.5 T. (b) The low frequency noise spectrum of MTJs with junction size 5 μm x 7.5 μm annealed under 0.5 T and 7 T fields in a helium environment.

Fig.4 The noise spectrum of MTJ bridge with junction size 10 μm x 15 μm annealed at 265°C under fields of 0.5 T and 7 T in a hydrogen environment. (The test sample was annealed at 265°C under fields of 0.5 T and 7 T and then annealed at 285°C under a field of 0.5 T in a helium environment before the hydrogen treatment.)

Fig. 5 A few design of magnetic flux concentrators (MFC)

Fig. 6 A picture of our MR sensor device with a ruler indicating its dimensions (about 2 inches long). The two bulk pieces lying on both sides of the MR sensor are magnetic flux concentrators. The MTJs was arranged as an asymmetry bridge in between the two magnetic flux concentrators

Fig. 7 Resistance (R) vs. Field curve of the MTJ with or without MFCs, showing the reversible field range (± 0.1 mT). It demonstrates that the signal of an MTJ bridge with magnetic flux concentrators increases by a factor of 77.

Fig. 8 The magnetic field detecting limit calculated from the noise spectrum of an MTJ sample with or without MFC

Fig. 9 Magnetic sensor output vs. field strength curve for different frequencies
The inset shows magnetic sensor output voltage under an ac magnetic field with frequency of 1 kHz and amplitude of 5 pT.

Fig. 10 Our prototype magnetoresistive sensor is operated by a set of coin-cell (3 volts) batteries. The operating power is less than 15 mW.

1. Introduction

This project is to develop highly sensitive magnetic sensors that fit the goal of the MMSON-07-03 Statement of Need. This need is to develop novel sensors applicable to the diverse detection and discrimination problems of munitions and explosives of concern (MEC) contaminated sites.

The objective of this project is to investigate a low-cost, practical magnetic sensor system suitable for high sensitivity magnetic field mapping, based on solid-state magnetic tunneling junction (MTJ) devices with a sensitivity in the picotesla (pT, 10^{-12} tesla) range at room temperature.

The measurement of magnetic field in the range of picotesla is important for a wide range of homeland security, industrial, scientific, and biomedical applications. Many of these applications require sensors with field noise of less than $1 \text{ nT/Hz}^{1/2}$ as well as low cost, small size, low frequency operation, low maintenance, and low power consumption. For example, there is need to develop novel sensor arrays to detect munitions and explosives of concern [1], monitor the change of magnetic field of earth and space [2], and detect magnetic biological signals and agents [3]. Currently the few sensors capable of detecting such small fields require cryogenic cooling such as SQUID sensors, require sophisticated detection systems such as atomic magnetometers and fluxgate magnetometers, or have large size and poor low frequency performance such as coil systems. [3-7]

The minimum detectable field (the field noise times the measurement bandwidth) of magnetic tunnel junction (MTJ) sensors is limited by thermal Johnson, shot, and intrinsic magnetic noise. However, due to extrinsic magnetic and barrier noise (which dominate at low frequencies) and non-reversible (hysteretic) behavior, current state-of-the-art MTJ devices have not demonstrated the desired performance [8-14]. The best detectable low-field of the commercial magnetoresistive magnetic field sensors studied by N. A. Stutzke *et. al* is on the order of 100 pT for frequencies below 10 Hz. [15].

In this project, we demonstrate a simple low-power, magnetic sensor system suitable for high sensitivity magnetic field mapping, based on solid-state MTJ devices with minimum detectable fields in the picotesla range at room temperature. The key features of this design are (1) decreasing the noise by the use of a 64 element bridge, (2) reducing the magnetic noise by annealing of MTJ in high magnetic field and a hydrogen environment, [16] and (3) increasing signal by using a external flux-to-field magnetic flux concentrators (MFC).

2. Fabrication of magnetoresistive sensor

In this study, we have addressed a few key issues that helped improve the sensitivity.

- (1) Sensor design--a 64 element bridge
- (2) Reduced magnetic noise by annealing of MTJ in high magnetic field and a hydrogen environment
- (3) Increased signal by using magnetic flux concentrators (MFC)

(1) Sensor design--a 64 element bridge

All the MTJs used in our study have the following structure: 5 nm Ta / 5 nm Cu / 10 nm $\text{Ir}_{20}\text{Mn}_{80}$ / 2 nm $\text{Co}_{90}\text{Fe}_{10}$ / 0.85 nm Ru / 3 nm $\text{Co}_{60}\text{Fe}_{20}\text{B}_{20}$ / 1.4 nm Al_2O_3 / 2 nm $\text{Co}_{90}\text{Fe}_{10}$ / 28 nm

$\text{Ni}_{80}\text{Fe}_{20} / 5 \text{ nm Ta} / 5 \text{ nm Ru}$ and have a resistance area product of approximately $RA = 10^5 \Omega \mu\text{m}^2$ and a tunneling magnetoresistance of about $\frac{\Delta R}{R} \times 100 = 45 \%$ where ΔR is the change in resistance between the parallel and antiparallel magnetization states and R is the resistance in the parallel state. The junctions were patterned into ellipses with a size of $13.3 \mu\text{m} \times 20 \mu\text{m}$ (area $209 \mu\text{m}^2$, eccentricity 0.74). The pinning direction of the reference layer is along the short axis of the ellipse. They were configured into 64 element symmetric bridges for noise measurements and asymmetric bridges (formed by taking two dies and rotating them so that the pinned directions were opposite to each other) for sensor measurements which is shown in Fig. 1 (a) and (b) respectively. (Note: All the MTJs used in our study are fabricated by Stephen E. Russek at NIST, Boulder.)

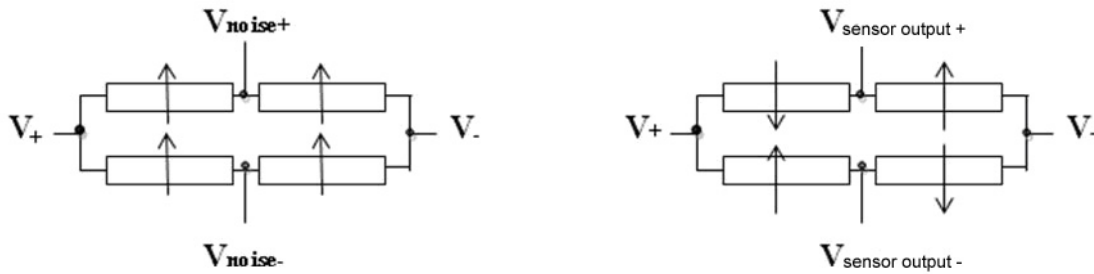


Fig. 1 (a) 64 element symmetric configuration (b) 64 element asymmetric configuration Arrows in the graph indicate the reference layer pinning direction.

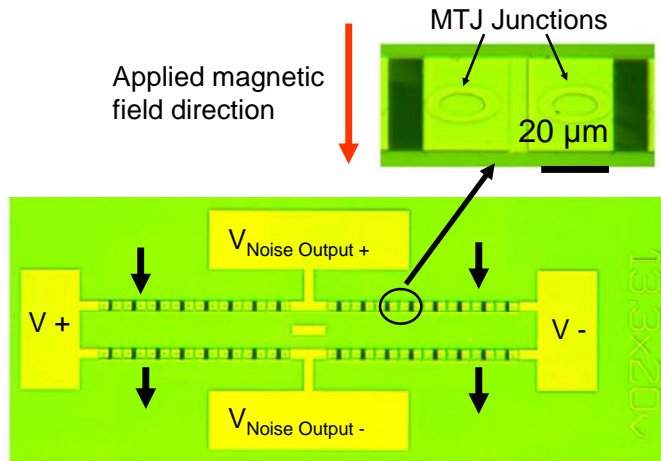


Fig. 2 The structure of the magnetic tunnel junctions (MTJs) is $5 \text{ nm Ta} / 5 \text{ nm Cu} / 10 \text{ nm Ir}_{20}\text{Mn}_{80} / 2 \text{ nm Co}_{90}\text{Fe}_{10} / 0.85 \text{ nm Ru} / 3 \text{ nm Co}_{60}\text{Fe}_{20}\text{B}_{20} / 1.4 \text{ nm Al}_2\text{O}_3 / 2 \text{ nm Co}_{90}\text{Fe}_{10} / 28 \text{ nm Ni}_{80}\text{Fe}_{20} / 5 \text{ nm Ta} / 5 \text{ nm Ru}$. The junctions were patterned into ellipses with a size of $13.3 \mu\text{m} \times 20 \mu\text{m}$ (area $209 \mu\text{m}^2$, eccentricity 0.75). They were configured into a 64 element symmetric configuration bridge. Solid arrows in the micrograph indicate the reference layer pinning direction for an symmetric bridge. The red arrow is the applied magnetic field direction.

(2) Reduced magnetic noise by annealing of MTJ in high magnetic field and a hydrogen environment

The noise measurement system is in a shielded environment to avoid picking up unwanted external magnetic field fluctuations. The sensor voltage and preamplifier bias are supplied by batteries to minimize noise. The MTJ sensor bridge was annealed at 265 °C under a 7 T magnetic field for 15 min in a hydrogen environment which have been demonstrated to reduce the noise level of the MTJs at low frequency [16].

First, we investigated the low frequency noise of an MTJ bridge with 5 μm x 7.5 μm ellipses annealed at 265 °C with different magnetic fields. As shown in Fig. 3(a), the magnetoresistance versus magnetic field curve shows that the MTJ annealed at 265 °C under a 7 T magnetic field is slightly less hysteretic than that of the one annealed at 265 °C under a 0.5 T magnetic field. As shown in Fig. 3(b), the sensors, after annealing at 7 T and 265 °C for 15 min and measured at 0 T bias field, show an improvement in the noise spectrum by about 2.5 times in the range of 1 to 10 Hz. There are only small changes at a higher frequency range (the small bump at about 20 Hz that deviates from the $1/f$ noise spectrum). These changes are related to the change of magnetic fluctuators in the MTJ due to annealing. The source of noise in MTJs can be magnetic or non-magnetic in origin, which can be distinguished by measuring under different magnetic fields. There is about an order of magnitude reduction of the low frequency noise spectrum when the MTJ measured under a 10 mT magnetic bias field. (Under this magnetic field the magnetization of free layer is parallel to that of the pinned layer.)

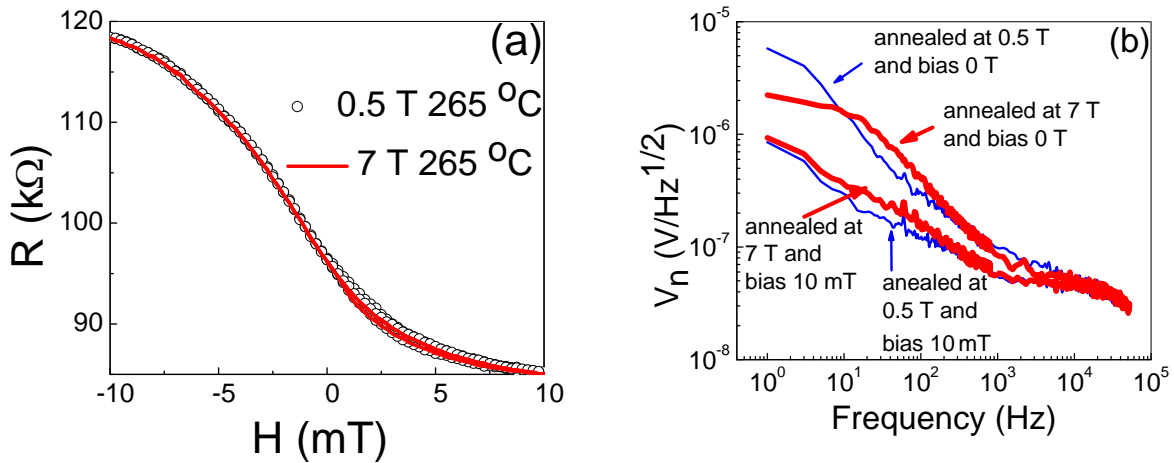


Fig. 3 (a) The R vs. H curve of the MTJ bridge with junction size 5 μm x 7.5 μm annealed at 265 °C under fields of 7 T and 0.5 T. (b) The low frequency noise spectrum of MTJs with junction size 5 μm x 7.5 μm annealed under 0.5 T and 7 T fields in a helium environment.

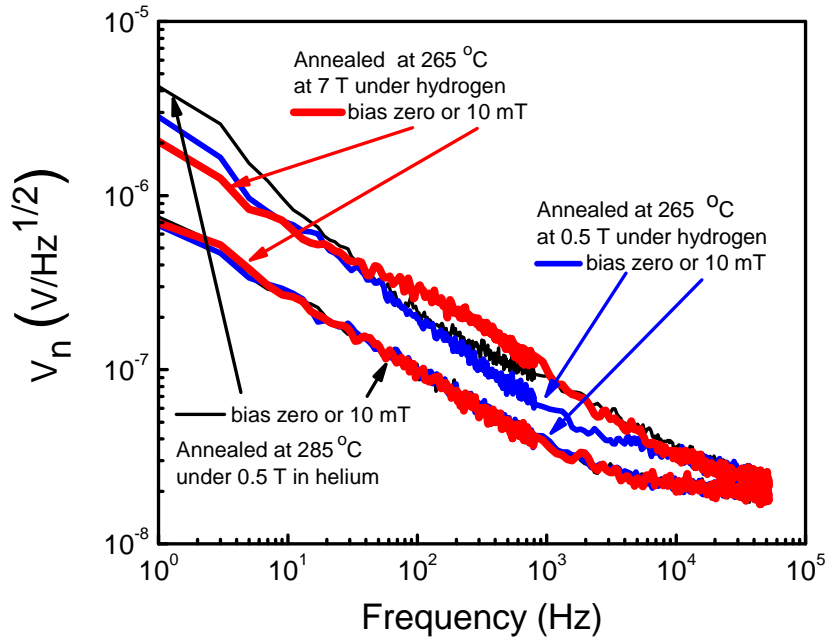


Fig.4 The noise spectrum of MTJ bridge with junction size $10\ \mu\text{m} \times 15\ \mu\text{m}$ annealed at 265°C under fields of 0.5 T and 7 T in a hydrogen environment. (The test sample was annealed at 265°C under fields of 0.5 T and 7 T and then annealed at 285°C under a field of 0.5 T in a helium environment before the hydrogen treatment.)

In order to reduce the noise level further, we have investigated the annealing of MTJ samples under a hydrogen atmosphere. In this study, we used the above MTJs (size $10\ \mu\text{m} \times 15\ \mu\text{m}$) that were already annealed at 285°C and under 0.5 T and then annealed them again in a different magnetic field under hydrogen gas at 265°C . As shown in Fig. 4, the noise level of the MTJ annealed under hydrogen gas and 0.5 T is reduced 2 times at low frequency (at 1 Hz) compared with the original sample (which was annealed at 285°C and under 0.5 T) and the noise level of the MTJ annealed under hydrogen gas at 7 T is reduced 3 times at low frequency (at 1 Hz) compared with the original sample. From the facts that there are only very small changes of the MR loop before and after hydrogen annealing of MTJ samples under high magnetic field, it indicates that there is no significant altering of the magnetization alignment of the AFM and FM layers at the interface. Hydrogen annealing of MTJ samples under high magnetic field may only remove some of the defects and change the pinning sites in the free layer as well as the pinning layer, which leads to the shift of magnetic fluctuators to higher frequencies and the reducing of the noise at low frequency. By optimizing the annealing temperature under H_2 , we may further improve the noise floor at low frequency in the future.

In summary, we have studied the low frequency noise of a few different sizes of MTJs in 64 element symmetric bridges. The noise of the MTJs at low frequency can be reduced by annealing under high magnetic field (7 T) and further improved by annealing in a hydrogen environment.

(3) Increasing signal by using magnetic flux concentrators:

The magnetic flux concentrator was made using a Conetic alloy which was annealed under hydrogen environment at 1150 °C for 20 hours with cooling rate about 1 °C/min.

A few design of magnetic flux concentrators (MFC) are shown in Fig 5. The gains of these MFC's are shown in Table 1.

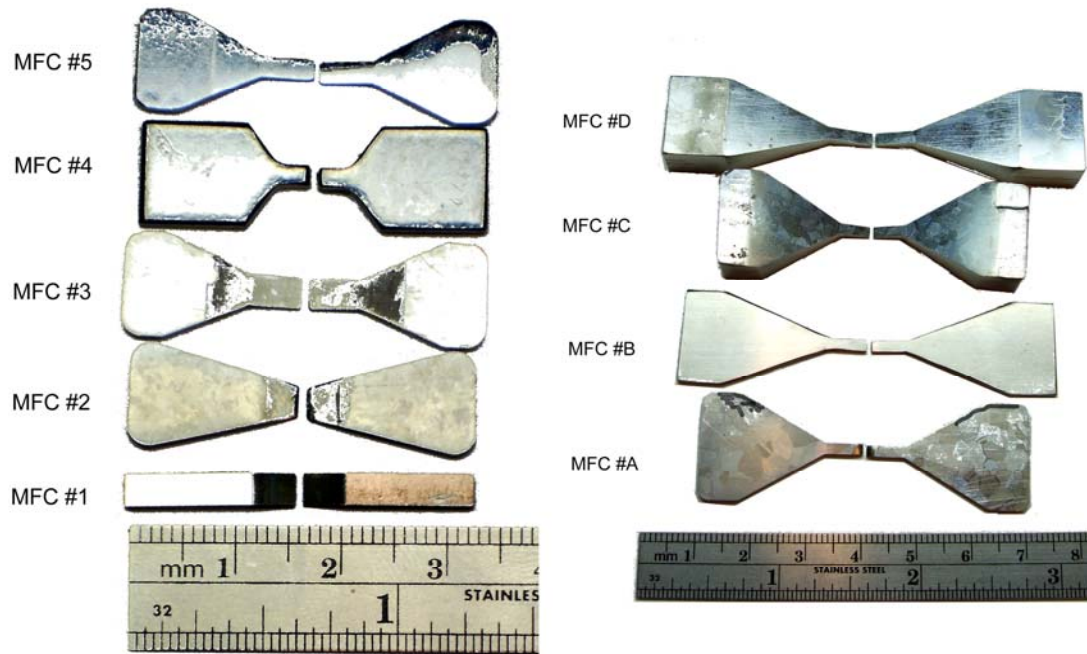


Fig. 5 A few design of magnetic flux concentrators (MFC)

Table 1 The estimated gains of various MFCs at gape of 1 mm

MFC	Gain
MFC#1	24
MFC#2	27
MFC#3	44
MFC#4	31
MFC#5	45
MFC#A	74
MFC#B	74
MFC#C	57
MFC#D	71

3. Magnetic sensor sensitivity

Fig. 6 shows a magnetic sensor with a pair of magnetic concentrators. The gap between the concentrators was typically 1 mm.

As shown in Fig. 7, the resistance of the MTJ bridge as a function of applied field, B , with and without MFCs. Without MFCs the percentage change with field is $\frac{\Delta R}{R\Delta B} \times 100 = 1.46\%/\text{mT}$ and it is increased to $113\%/\text{mT}$ with a MFC. Thus, the MFCs provide a 77-fold magnification of the flux density.

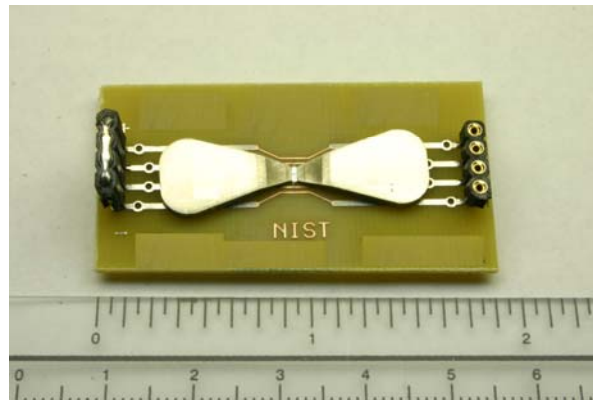


Fig. 6 A picture of our MR sensor device with a ruler indicating its dimensions (about 2 inches long). The two bulk pieces lying on both sides of the MR sensor are magnetic flux concentrators. The MTJs was arranged as an asymmetry bridge in between the two magnetic flux concentrators

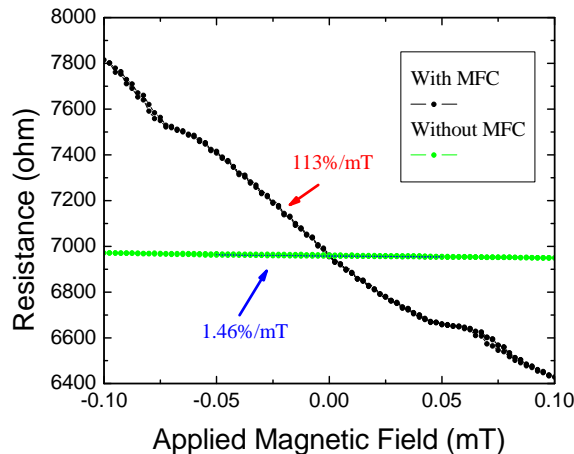


Fig. 7 Resistance (R) vs. Field curve of the MTJ with or without MFCs, showing the reversible field range (± 0.1 mT). It demonstrates that the signal of an MTJ bridge with magnetic flux concentrators increases by a factor of 77.

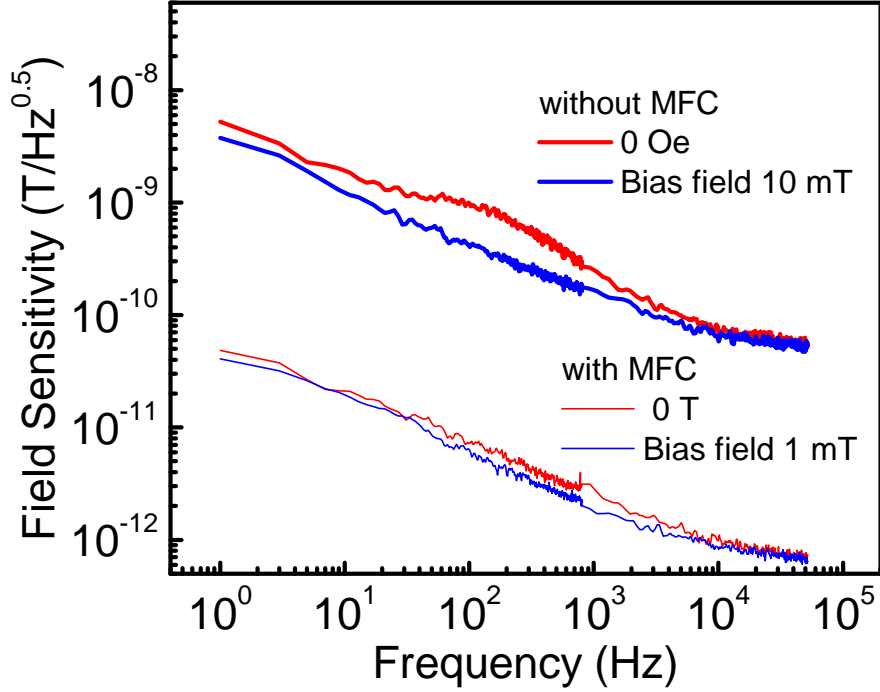


Fig. 8 The magnetic field detecting limit calculated from the noise spectrum of an MTJ sample with or without MFC

We measured the field noise of the MTJ bridge in the frequency range from 1 to 5×10^4 Hz with and without MFCs and biasing fields, as shown in Fig. 8. The magnetic field noise was calculated by dividing the voltage noise spectrum measured at the bridge outputs by the bridge sensitivity $I dR/dB$ taken from Fig. 7. At an applied voltage of 10 V across the bridge and zero applied field, the sensitivity is 11300 V/T. Since the noise level at 1 Hz is $0.5 \times 10^{-6} \text{ V/Hz}^{1/2}$, the field noise is $0.5 \times 10^{-6} \text{ V/Hz}^{1/2} / 11300 \text{ V/T} = 44 \text{ pT/Hz}^{1/2}$. At 10 Hz, the noise level is $1 \times 10^{-8} \text{ V/Hz}^{1/2}$, and the field noise is $1 \times 10^{-8} \text{ V/Hz}^{1/2} / 11300 \text{ V/T} = 0.9 \text{ pT/Hz}^{1/2}$. At high frequencies the field noise is limited by the Johnson, shot, and intrinsic thermal magnetic noise. The calculated intrinsic magnetic noise for this sensor at 100 kHz are $0.86 \text{ pT/Hz}^{1/2}$ and $66 \text{ pT/Hz}^{1/2}$ with and without the MFC respectively. These calculated numbers agree well with the extrapolated data shown in Fig. 8 which give intrinsic field noise of $0.66 \text{ pT/Hz}^{1/2}$ and $50 \text{ pT/Hz}^{1/2}$ respectively. The shot noise, which is the largest source of intrinsic noise, scales $\frac{1}{\sqrt{N}}$

where N is the number of elements in each leg of the bridge. Hence, the intrinsic noise is reduced by a factor of four by using a bridge in which each leg consist of 16 serial junctions. As shown in Fig. 8, integration of MFCs into MTJs greatly reduces the field noise. The MFCs do not produce extra noise since only small changes were observed in the voltage noise spectrum of the MTJ bridge with and without MFCs. Hence, the improvement in the field noise is solely a result of the increase in sensitivity arising from the flux concentrators. For the noise spectrum of MTJ without MFC shows a small bump near 200 Hz that deviates from the $1/f$ noise spectrum, as shown in the top of Fig. 8. With MFC, this magnetic fluctuator (the small bump at 200Hz in the

noise spectrum) in the MTJ disappears possibly due to the magnetic interactions between the MFC and the free layer. We have measured the noise spectrum under different magnetic fields to distinguish the magnetic and nonmagnetic components of the noise in MTJs. There are only small differences in the noise spectrum when the MTJ sensor is measured under a 10 mT magnetic bias field (under this magnetic field the magnetization of free layer is parallel to that of the pinned layer.). This indicates that the magnetic noise magnitude is on the same order as the nonmagnetic noise, which is presumed to arise from fluctuations in the tunnel barrier. The magnetic noise in this sensor is significantly reduced by our annealing process similar to results presented in Ref. 16.

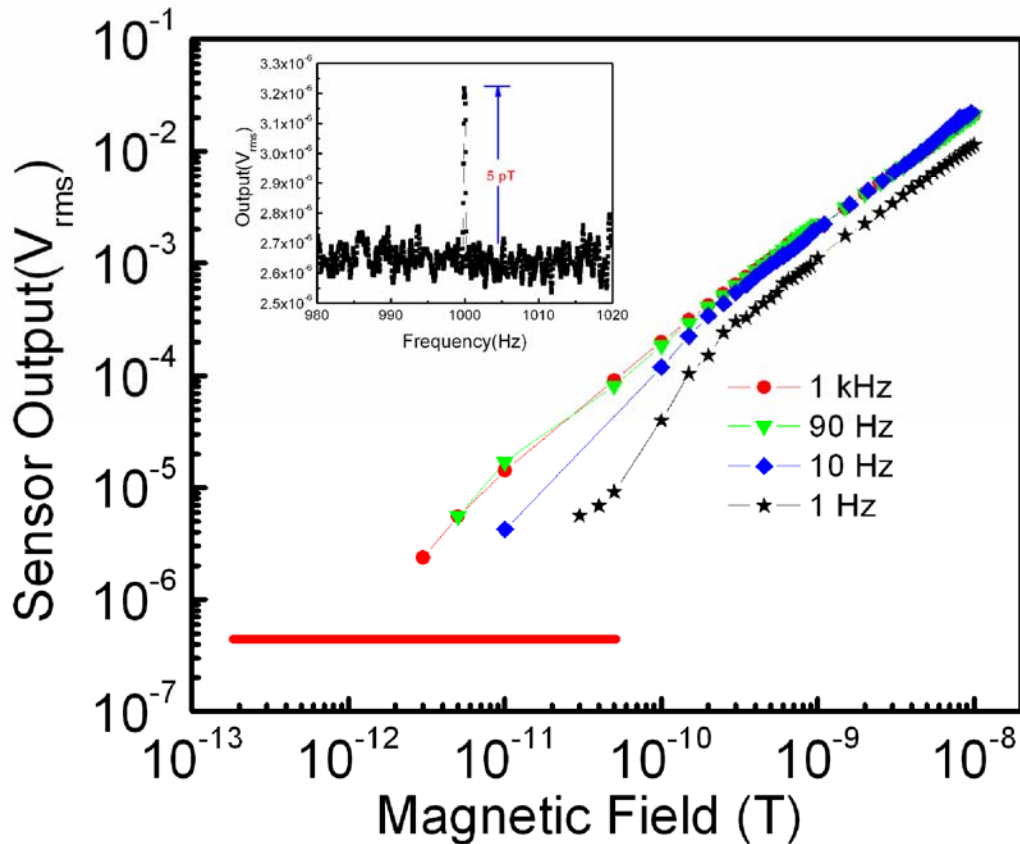


Fig. 9 Magnetic sensor output vs. field strength curve for different frequencies
The inset shows magnetic sensor output voltage under an ac magnetic field with frequency of 1 kHz and amplitude of 5 pT.

The performance of this sensor, for various applied field strengths and frequencies, is shown in Fig. 9. The inset of Fig. 9 shows one of the measurements. An ac magnetic field with frequency of 1 kHz and amplitude of 5 pT was generated by a Helmholtz coil driven by a function generator and a precision current source. The magnetic sensor was placed inside the Helmholtz

coil and the signal was collected by a vector signal analyzer with a low noise amplifier (gain was set at 10^3). The magnetic sensor under an ac magnetic field with frequency of 1 kHz and amplitude of 5 pT has an output of about 6 μV . The sensor output vs. field strength curve for different frequencies is shown in Fig. 9. The data were taken, for a given resolution bandwidth on the spectrum analyzer, until the signal disappeared into the background. The lowest field point for each frequency is an approximate measure of the minimum detectable field and gives 3 pT, 10 pT and 30 pT at 1 kHz, 10 Hz, and 1 Hz respectively. The red bar indicates the limit of our sensor assuming no extrinsic noise sources, just the intrinsic noise sources discussed above. The results are consistent with what we calculated from the noise spectrum and the signal output which predicts a minimum detectable field in a 1 Hz bandwidth of 1 pT, 5 pT and 50 pT at 1 kHz, 10 Hz, and 1 Hz respectively. The resistance of our magnetic sensor is about 7 kohm so that the sensor only dissipates about 15 mW of power while operating at 10 V applied voltage.

4. Summary

In summary, we present a low power, compact, magnetoresistive sensor that combines a 64 element magnetic tunnel junction bridge and a set of low noise magnetic flux concentrators, as shown in Fig. 10. Sensitivity in the range of a few picotesla has been achieved. Magnetic field sensitivities of our prototype magnetic sensor are about $1 \text{ pT/Hz}^{1/2}$ at 1 kHz, $5 \text{ pT/Hz}^{1/2}$ at 10 Hz, and $50 \text{ pT/Hz}^{1/2}$ at 1 Hz. The magnetic sensor only dissipates 15 mW of power while operating.

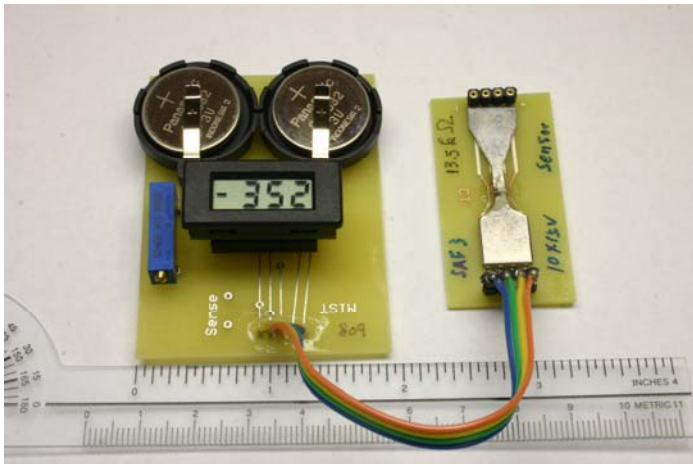


Fig. 10 Our prototype magnetoresistive sensor is operated by a set of coin-cell (3 volts) batteries. The operating power is less than 15 mW.

In the future, further improvements of MTJ sensors for operation in the femtotesla (fT, 10^{-15} tesla) range at room temperature are possible. It can be achieved by using (1) new MgO based tunneling junctions (a TMR ratio of 500% [17]), (2) a better design of magnetic flux concentrator (a gain of 300 [18]), and (3) optimized stack deposition conditions and annealing procedures to eliminate defects giving rise to $1/f$ noise. It has been shown that proper annealing reduces magnetic noise by about an order of magnitude in MgO based tunneling junctions [19].

A possible road map for magnetic devices to achieve sensitivity in the femtotesla (fT, 10^{-15} tesla) range at room temperature is as follows:

1. MTJ with MR ratio >550% TMR change => improve sensitivity by 10 - 50 (The MR ratio of the current MTJ sensor with a sensitivity in the picotesla (pT, 10^{-12} tesla) range at room temperature is only 45% TMR change.)
2. Magnet nanostructure => single, stable domain => reduced noise by 10 - 100 (This can be achieved by improving further our annealing procedures.)
3. Ultra-soft magnetic layer => Magnetization easier to rotate => improve sensitivity by 10 - 50 (This can be achieved by modified magnetic free layer structures.)
4. Magnetic concentrator => improve sensitivity by 10 -1000 (This can be achieved by using amorphous alloys such as magnetic alloy 2705M which has about two order of magnitude higher permeability than the one we used now.)

If we are able to implement most of these improvements we will have for opportunity to improve the sensitivity of magnetic devices by $10^3 - 10^5$!!

5. References:

1. David J. Wright and Jim Kingdon, "Development of a Combined EMI/Magnetometer Sensor for UXO Detection," Proc. Symposium on the Applications of Geophysics to Environmental and Engineering Problems (SAGEEP), Colorado Springs, Feb. 22-26, 2004, pp. 1805-1814.
2. Jeffrey J. Love, "Magnetic Monitoring of Earth and Space", Phys. Today, **vol. 61**, No.2, pp31, (2008)
3. Karsten Sternickel and Alex I Braginski, Supercond. Sci. Technol. **19**, S160-S171 (2006)
4. Dmitry Budker and Michael Romalis, Nature Physics **Vol 3**, p227 (2007)
5. Peter D. D. Schwindt, Brad Lindseth, Svenja Knappe, Vishal Shah, and John Kitching, and Li-Anne Liew, Appl. Phys. Lett., **90**, 081102 (2007)
6. Vishal Shah, Svenja Knappe, Peter D. D. Schwindt, John Kitching, Nature Photonics **1**, L649 - L652 (2007)
7. R. H. Koch and J. R. Rozen, Appl. Phys. Lett., **78**, 1897 (2001)
8. J. M. Almeida, P. Wisniowski, and P. P. Freitas, J. Appl. Phys., **103**, 07E922 (2008)
9. P. P. Freitas, R. Ferreira, S. Cardoso, and F Cardoso, J. Phys.: Condens. Matter., **19**, 165221 (2007)
10. Dipanjan Mazumdar, Xiaoyong, Xiaoyong Liu, Dipanjan Mazumdar, Weifeng Shen, B. D. Schrag, and Gang Xiao Appl. Phys. Lett., **89**, 023504 (2006)
11. J. Scola, H. Polovy, C. Fermon, M. Pannetier-Lecoecur, G. Feng, K. Fahy, and J. M. D. Coey, Appl. Phys. Lett., **90**, 252501 (2007).
12. R. C. Chaves, P. P. Freitas, Ocker and W. Maass, Appl. Phys. Lett., **91**, 102504 (2007).
13. J. M. Almeida, R. Ferreira, P. P. Freitas, J. Langer, B. Ocker, and W. Maass, J. Appl. Phys., **99**, 08B314 (2006).

14. Dipanjan Mazumdar, Xiaoyong Liu, B. D. Schrag, Weifeng Shen, Matthew Carter, Gang Xiao, J. Appl. Phys., **101**, 09B502 (2007)
15. N. A. Stutzke, S. E. Russek, D. P. Pappas, and M. Tondra, J. Appl. Phys., **97**, 10Q107 (2005).
16. S. H. Liou, Rui Zhang, Stephen E. Russek, L. Yuan, Sean T. Halloran, and David P. Pappas, J. Appl. Phys., **103**, 07E920 (2008)
17. Y. M. Lee, J. Hayakawa, S. Ikeda, F. Matsukura, and H. Ohno, Appl. Phys. Lett., **90**, 212507 (2007)
18. Predrag M. Drljača, Frank Vincent, Pierre-André Besse, Radivoje S. Popović, Sensors and Actuators **A 97-98**, 10-14 (2002)
19. F. G. Aliev, R. Guerrero, D. Herranz, R. Villar, F. Greullet, C. Tiusan, and M. Hehn, Appl. Phys. Lett., **91**, 232504 (2007)

6. Appendices:

Publications:

1. S. H. Liou, Rui Zhang, Stephen E. Russek, L. Yuan, Sean T. Halloran, and David P. Pappas, “Dependence of noise in magnetic tunnel junction sensors on annealing field and temperature”, J. Appl. Phys., **103**, 07E920 (2008)

Presentations:

- (1) “Dependence of noise in magnetic tunnel junction sensors on annealing field and temperature”, S. H. Liou, Rui Zhang, Stephen E. Russek, L. Yuan, Sean T. Halloran, and David P. Pappas, submitted to 52nd Annual Conference on Magnetism and Magnetic Materials, 2007
- (2) “Noise study of magnetic tunnel junction sensors with magnetic flux concentrators” S. H. Liou, Stephen E. Russek, L. Yuan, Sean T. Halloran, and David P. Pappas, the poster will presentation at 2007 Partners in Environmental Technology Technical Symposium & Workshop, December 4-6)